JOURNAL OF MATERIALS SCIENCE: MATERIALS IN MEDICINE 4 (1993) 50–54

High-strength biofunctional zirconia: mechanical properties and static fatigue behaviour of zirconia–apatite composites

J. LI, L. HERMANSSON, R. SÖREMARK
Center for Dental Technology and Biomaterials, Karolinska Institute, Box 4064, S-141 04 Huddinge, Sweden

Zirconia and zirconia–apatite (hydroxyl- and fluor-) composites were sintered at 1225 °C by glass-encapsulated hot isostatic pressing. In addition to the general assessment of the mechanical properties of the materials, the static fatigue behaviour of the zirconia–hydroxylapatite composite was evaluated by measuring the slow crack propagation at different loads in a circulating 0.9% NaCl solution at 37 °C. The mean fracture strengths of the materials in three-point bending mode were 770, 860 and 910 MPa for zirconia–fluorapatite, zirconia–hydroxylapatite and zirconia, respectively. The high value of the slow crack growth stress exponent, calculated from the average strength at the different loading rates, indicates that the zirconia–hydroxylapatite has excellent fatigue resistance in addition to high strength. The even distribution of the apatite phases as islets in the zirconia matrix may contribute to mineralization and direct bone apposition to this type of ceramic composites. The machinability of zirconia materials is discussed.

1. Introduction

Partially stabilized zirconia has been of interest as a structural ceramic, due to its high strength and improved fracture toughness compared with other ceramics. Yttria-doped (3 mol %) tetragonally stabilized zirconia (TZ3Y) exhibits a strength level measured by three-point bending as high as 1–2 GPa [1–3]. These data have expanded the application sphere for zirconia to the medical field as an implant material. Orthopaedic implants (hip-joint prostheses) and dental implants (blades) are commercial examples [4, 5]. The high strength has inspired orthopaedics to use zirconia hip-joint heads with reduced head diameter of 22 mm instead of 32 mm to reduce the relative movement of the hip joint. The relatively low Young's modulus of zirconia materials compared with alumina may facilitate the retention of the implant in cortical bone. Histological evaluation indicates the biocompatibility of zirconia to be similar to that of alumina [6].

The application field of zirconia may be further extended by introducing a bioactive phase into the zirconia matrix by analogy with what has been recently proposed for other oxide systems [7–10]. The bioactive phase, hydroxylapatite (HA) or fluorapatite (FA), may be introduced in such a way that it influences the strength minimally, i.e. by selecting the size of the HA or FA phase areas that is smaller than the critical strength-controlling defect size of the system. In this study zirconia and zirconia–apatite composites were densified by glass-encapsulated hot isostatic pressing (HIPing) using the ABB Cerama AB technique [11] at 1225 °C. In addition to a general assessment of the mechanical properties of the systems, the fatigue (the slow crack growth behaviour) of one of the composite materials was evaluated. The significance of improved fatigue properties to the safety of implant materials based on zirconia was analysed, as well as the machinability behaviour of zirconia materials.

2. Materials and methods

2.1. Powder preparation and densification

Submicrometre powders of HA and TZ3Y manufactured by Merck and Toyo Soda, respectively, were used. FA was synthesized by heating CaF_2 (1 mol) and $Ca_3(PO_4)_2$ (3 mol) at 1000 °C for 4 h and then grinding for 48 h and sieving through a sieve cloth of 3 μm openings. The powder mixtures were ground by ball-milling in light benzine for 48 h (silicon nitride balls and polyethylene container) and subsequently sieved through a 10 μm sieve cloth to improve the homogeneity. In one composition a coarse HA powder was used, and in this case sieving was omitted. A description of the powders is given in Tables I and II.

The powders were cold isostatically pressed at a pressure of 250 MPa for 10 min. The pressing yielded a density of approximately 58% of the theoretical compact density. The green bodies were subsequently glass-encapsulated and densified by HIPing at 160 MPa for 1 h at the top temperature of 1225 °C and then cooled to room temperature at a cooling rate of 1 °C min^{-1}.

0957–4530

TABLE I Physical properties of the powders studied

Powder	Specific surface area ($m^2 g^{-1}$)[a]	Grain size (μm)
Hydroxylapatite (HA)	36	$\ll 1$
Zirconia (TZ3Y)	18	< 0.3
Fluorapatite (FA)	n.d.[b]	< 3[c]

[a] Determined by the Brunauer–Emmett–Teller method.
[b] Not determined.
[c] Sieved.

TABLE II Compositions of the materials studied

Code	Composition
TZ3Y	100% TZ3Y
TZ3Y–HA	85% TZ3Y–15% HA
TZ3Y–FA	75% TZ3Y–25% FA
TZ3Y–HAL[a]	75% TZ3Y–25% HAL

[a] HAL, HA with large grain size (> 50 μm).

TABLE III Physical and mechanical properties of the sintered materials

Code	Density ($g\ cm^{-3}$)	Hardness (GPa)	Three-point bending strength (MPa)	Weibull modulus, m	Fracture toughness ($MPa\ m^{1/2}$)
TZ3Y	6.05	12.9 ± 0.3	910	14	> 5[a]
TZ3Y–HA	5.64	12.3 ± 0.3	860	11	4.6
TZ3Y–FA	5.34	12.5 ± 0.5	772	12	4.5
TZ3Y–HAL	5.35	10.6 ± 0.5	217	6	3.2

[a] No detectable cracks were recorded under load of 10 N.

2.2. Evaluation of physical and mechanical properties

The density of sintered samples was determined by the Archimedes method. The bending strength was determined by using the three-point bending technique on cut and chamfered samples of the geometry 3.5 mm × 3.5 mm × 30 mm at a crosshead speed of 0.5 mm min^{-1} (Alwetron 50). Ten to 20 test bars of each material were used. The Vickers hardness and fracture toughness were measured by the indentation technique using a Shimadzu microhardness tester at loads of 5 and 10 N, respectively.

The slow crack propagation was characterized for one of the composite materials by determining the slow crack growth stress exponent (n). The n-value was obtained by measuring the bending strength (mean of five samples) at different crosshead speeds (Instron 8561). The experiments were carried out in a circulating 0.9% NaCl solution at 37 °C. The relationship

$$\ln \sigma_f = B + [1/(n+1)]\ln(d\sigma/dt)$$

was used, where σ_f is the mean bending strength at given stress rate $d\sigma/dt$.

The general microstructure, fracture surface and microstructure developed during slow crack growth were observed in a scanning electron microscope (SEM).

3. Results and discussion

The general mechanical data obtained for the materials presented in Table II are shown in Table III. As can be seen, all materials were densified to more than 99% theoretical. The mechanical strengths of the composite materials were almost as high as that of pure zirconia and considerably higher than those of the alumina ceramics often used in the clinic [12]. An even distribution of the second phase is of vital interest to maintain a high strength of the composite materials. Only a minor reduction in the strength compared with the pure zirconia was obtained for the fine-grained composite materials. The apatite phases were evenly distributed in the zirconia matrix as islets (spots), see Figs 1 and 2. The average size was well below 5 μm. The low mechanical strength of the material TZ3Y–HAL reflected the large grain size of HA phase in this case.

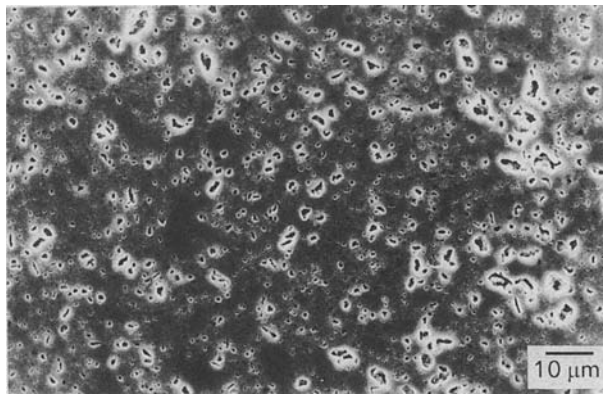

Figure 1 Scanning electron micrograph of TZ3Y–HA composite, overetched. The pores originate from the HA grains which were etched away.

Fracture surface area analyses showed apatite grains (about 10–20 μm in size) to be the main fracture origin in the fine-grained zirconia–apatite composites. The somewhat lower values of the Weibull modulus (m) obtained for the composite materials, compared with pure zirconia, are related to the spread of the size of the apatite grains. The fracture toughness values of the composite materials were low in comparison with

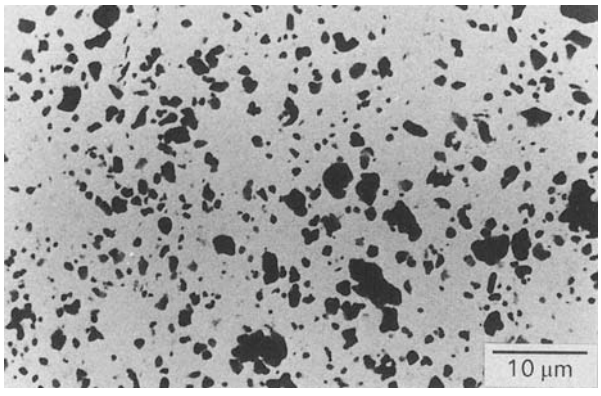

Figure 2 Backscattered electron imaging micrograph of TZ3Y–FA, showing the distribution of the apatite phase in zirconia matrix. Dark areas are fluorapatite.

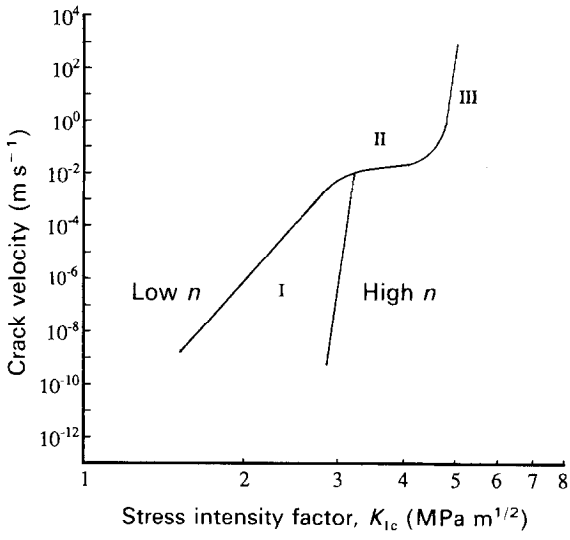

Figure 4 v–K_I dependence for ceramic materials.

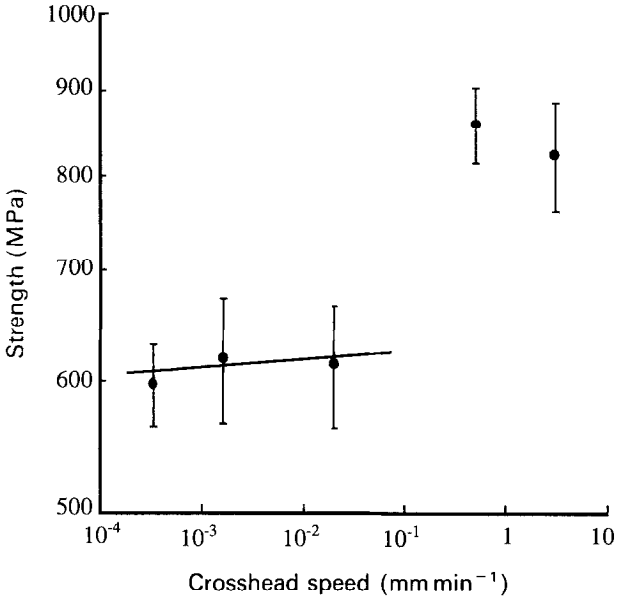

Figure 3 Fracture strength of TZ3Y–HA at different loading rates.

literature data for zirconia materials. This may be due to the very fine grain size of the HIPed zirconia matrix, as discussed by Lepistä *et al.* [13]. The introduction of the apatite phase, as well as the use of a low sintering temperature, reduces the grain growth. The low sintering temperature (1225 °C) was chosen to avoid possible decomposition of the apatite phase. X-ray diffraction measurements confirmed the presence of the apatite phase in the processed materials.

The slow crack growth results for the composite TZ3Y–HA are presented in Fig. 3. Data calculated based on the three lowest loading rates (linear regression) correspond to an n-value of > 100, which is higher than most values reported for oxides [14]. A break point is obtained at high loading rates. This is probably caused by a high influence of region II (and III) behaviour in the general v–K_I relationship [15] (Fig. 4). The contribution of crack propagation in region I is extremely small. The accuracy of the n-value, however, is low since only three loading rates could be used due to the break point, but it is evident that the n-value is high. In fact, data infer a stress threshold value of the crack propagation in the interval 500–600 MPa. Crack propagation in region II and maybe in region III is highly dependent on the loading rate. Low loading rates yield sufficient time for propagation, whereas rapid loading reduces the crack propagation and the final crack length, with the resultant higher ultimate strength. High n-values in addition to high m-values are essential in assuring safe structural (high-strength) ceramics, i.e. very low probability of rapid fracture as well as delayed fracture up to half the average fracture stress [16, 17]. The result indicates that the composite has a high reliability as far as the static fatigue behaviour is concerned.

Evaluation of the microstructure in the fracture region of materials (Figs 5 and 6) indicates a similar intergranular fracture pattern to be the main mode for both rapid and delayed fracture. The strength of the individual zirconia grains is probably very high due to the extremely small size of the grains (approximately 0.2 μm in diameter), thus favouring intergranular fracture. The similar fracture pattern for rapid and delayed fracture also supports the finding of a high n-value for the TZ3Y–HA composite. A high fatigue resistance of the TZ3Y–FA composite is also likely, since the zirconia matrix seems to control both the strength and the crack propagation behaviour.

The zirconia–apatite composites may extend the application of zirconia in the biological field, due to possible bioactivity of the HA- or FA-containing ceramics. The microstructure of the composites showed that the apatite phase was evenly distributed in the zirconia matrix, with most spots below a few μm in size. The high n-value of the TZ3Y–HA composite material is thus strongly related to the matrix and not to the weak HA-phase. Furthermore, these apatite spots may play an important role in facilitating bone apposition during new bone growth. The related biological evaluation including cytotoxicity, histology and bonding strength developed between this type of ceramics and the bone will be presented elsewhere.

Observations from the test bar preparation of the materials in this study, as well as other ceramics (cutting, chamfering and chipping), are worth mentioning. It was found that the ease of machining

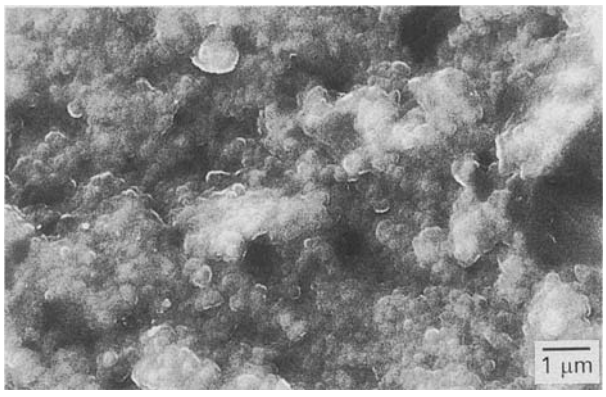

Figure 5 Scanning electron micrograph of the fracture surface of TZ3Y–HA composite, rapid fracture, intergranular fracture.

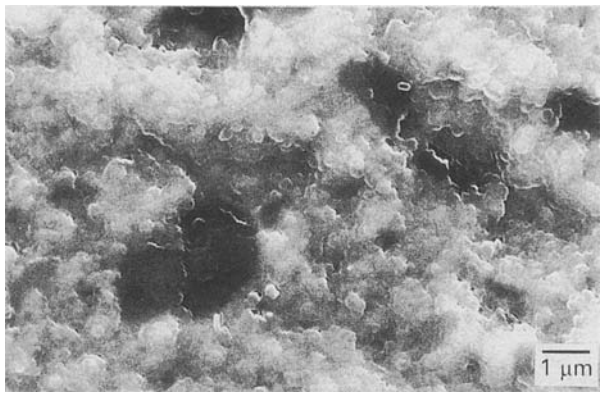

Figure 6 Scanning electron micrograph of the fracture surface of TZ3Y–HA composite, delayed fracture, intergranular fracture.

TABLE IV Machinability performance index of ceramics [MPIC = $(K_{Ic}/E) \times 10^5$]

	SiC	Si_3N_4	Sialon	HA	Al_2O_3	ZrO_2[a]	TiO_2	Al_2O_3(SiC Wh[b])
K_{Ic}	3.5	5.0	5.5	1.1	4.0	4.7	2.8	6
E	410	330	300	100	385	210	270	390
MPIC	< 1	1.5	1.8	1.0	1.0	1.9–3.3	1.0	1.5

[a] Data from this study and from the literature [1, 7, 8, 11, 15, 18, 19].
[b] Wh, 15–20 vol % whisker.

test bars (avoiding severe chipping) was strongly related to two physical properties: the fracture toughness and the Young's modulus. Due to the considerably lower Young's modulus compared with most structural ceramics, the zirconia materials studied showed good machinability in spite of a relatively low K_{Ic} in the case of the composites. A machinability performance index of ceramics (MPIC) is proposed as $(K_{Ic}/E) \times 10^5$. Data from this study and from the literature [1, 7, 8, 11, 15, 18, 19] are compiled in Table IV. In order to reduce the probability of severe machining defects, ceramics with high MPIC values (> 1.5) should be preferred. Materials based on zirconia emerge as the main candidates for structural devices including highly loaded implants for biomedical applications.

4. Conclusions

1. Zirconia and its HA- and FA-composites were virtually fully densified by glass-encapsulated HIPing at a relatively low temperature (1225 °C).

2. The strength level of the fine-grained materials was 770–910 MPa with fracture toughness > 4.5 MPa $m^{1/2}$.

3. Evaluation of the static fatigue behaviour showed the zirconia–HA composite to have excellent slow crack growth resistance ($n > 100$).

4. The machinability of zirconia and zirconia composites compared with other ceramics is facilitated by high strength and fracture toughness related to relatively low E-modulus and hardness values.

Acknowledgements

The authors express their gratitude for partial financial support by the Swedish National Board for Technical Development. We thank Professor David Rowcliffe for permission to use the mechanical testing facilities at the Royal Institute of Technology, Stockholm. The SEM work by Lars Eklund at the Swedish Ceramic Institute and the English revision by Myra Flores are gratefully acknowledged.

References

1. A. K. TJERNLUND, L. HERMANSSON, K. ARVIDSON and R. SÖREMARK, *Sci. Ceram.* **14** (1988) 799.
2. K. TSUKUMA, K. UEDA and T. TSUKIDATE, European Patent 0 140 638, A1 (1985).
3. T. YEN and J. GUO, in "Advances in ceramics", Vol. 24B, edited by S. Somiya, N. Yamamoto and H. Yaragida (American Ceramic Society, Westerville, Ohio, 1988) p. 573.
4. T. MINAMIZATO, *J. Prosthet. Dent.* **63** (1990) 677.
5. Desmarquest, Prozyr, Technical data sheet (1990).
6. P. S. CHRISTEL, in "Concise encyclopedia of medical and dental materials", edited by D. Williams (Pergamon Press, London, 1990) p. 375.
7. J. LI, B. FARTASH and L. HERMANSSON, *Interceram* **39** (1990) 20.
8. J. LI, S. FORBERG and L. HERMANSSON, *Biomaterials* **12** (1991) 438.
9. K. IOKU, M. YOSHIMURA and S. SOMIJA, *ibid.* **11** (1990) 57.
10. G. RIESS and A. GEIGER, German Patent DE-A-29 28 007 (1987).
11. H. T. LARKER, in "Progress in nitrogen ceramics", edited by F. L. Riley (Martinus Nijhoff, The Hague, 1983) p. 719.
12. G. ANNEROTH, A. R. ERICSSON and L. ZETTERQVIST, *Swed. Dent. J.* **14** (1990) 63.

13. T. LEPISTÄ, T. MÄNTYLÄ, G. GUNNARSSON, E. L. SVEINSDOTTIR and A. K. WESTMAN, in Proceedings of the 1st European Ceramic Society, edited by E. De With, R. A. TERPSTRA and R. METSELAAR, Vol. 3 (Elsevier, London, 1989) p. 3458.
14. M. V. SWAIN and V. ZELIZKO, in "Bioceramics", Vol. 2, edited by G. Heimke (Heidelberg, 1990) p. 135.
15. U. SOLTESZ and H. RICHTER, in "Metal and ceramic biomaterials", Vol. II: "Strength and surface", edited by P. Ducheyne and G. W. Hastings (CRC Press, Boca Raton, Florida, 1984) p. 46.
16. L. HERMANSSON, "Guidelines for use and design with ceramics" (in Swedish) in press.
17. A. P. NIKKILÄ and T. MÄNTYLÄ, Presented at American Ceramic Society Meeting, Engineering Ceramics Division, Cocoa Beach, 16 January 1989.
18. N. HECHT, *Ceram. Engng Sci. Proc.* **9** (1988) 1313.
19. Sandvik Hard Materials AB, Stockholm, Technical data sheet (1991).

Received 2 September
and accepted 26 November 1991